

The flood case 27–29 July 2004: added value of the meso- γ -scale HIRLAM?

SAMI NIEMELÄ and THOMAS LORIDAN*

Finnish Meteorological Institute, P.O.Box 503, FI-00101 Helsinki, Finland

1 Introduction

The southern and central parts of Finland received very large precipitation amounts during 27–29 July 2004. This rain event caused flooding over large areas. Radar retrieved 12-hour accumulated precipitation amounts are showed in Fig. 1, which roughly illustrates the development of the event. A slowly moving low pressure system approached southern Finland between 12 UTC 27 July and 12 UTC 28 July. During 28 and 29 July the low pressure center remained nearly stationary over Gulf of Finland. Consequently, a large and locally very intense precipitation area (over 50 mm 12h⁻¹ in Fig. 1b) travelled across southern and central Finland towards Kainuu. While the low pressure system remained over the Gulf, the rain area rotated back across the central Finland due to upper-air flow by the same path as it came. This resulted in a record breaking diurnal precipitation amount, 122 mm in 24 hours, measured at Vesanto, central Finland (location marked with black dot in Fig. 2), on 06 UTC 29 July 2004.

The reference HIRLAM, ran operationally at FMI with a horizontal resolution of 22 km (RCR), failed to produce such strong precipitation amounts as were observed. In general, the intensity of strong convective rain is not adequately represented by large-scale models. Accordingly, the development of meso- γ -scale (2–20 km after Orlanski, 1975) numerical weather prediction (NWP) models is a very current issue. These models cannot resolve individual convective elements, but they can resolve organized mesoscale convective systems or squall lines.

The objective of this study is to clarify the following questions. Can we simulate the structure of the precipitation event with meso- γ -scale HIRLAM? Can we even make better precipitation forecasts by just reducing the grid length? In this study, we also compare the nonhydrostatic version of HIRLAM (Rõöm, 2001) with the traditional hydrostatic HIRLAM.

The different model configurations are validated using data from FMI's radar network. Modelled radar reflectivities from non-operational experiments are computed by using the Radar Simulation Model (RSM) of Haase and Crewell (2000). RSM is a software package, that simulates radar reflectivity measurements corresponding to the output of a NWP model (Haase and

*Intern from MATMECA, University of Bordeaux, during Jun–Aug 2004

Fortelius, 2001). As a result, it is possible to validate the model results by comparing the modelled radar reflectivities with the actual radar reflectivity measurements. Another benefit of RSM is that the modelled and observed reflectivities are presented by the same observation geometry.

2 Experimental setup

Several experiments, both simulations and forecasts, are conducted in order to study the extreme precipitation event. In addition, FMI’s operational forecast results are also used in the evaluation. At this point, it is important to emphasize the difference of the terms *forecast* and *simulation*. Forecast is a model integration, in which the boundary fields are also forecasts. However, in simulations the boundaries are not true forecasts. In our simulations the lateral boundaries are analyses from a coarser resolution model. In this way we try to ensure that the dynamical forcing during the simulation is as good as possible, so that the model results and observations would be more comparable. Consequently, the behaviour of experiments is easier to interpret.

Table 1 describes all the model configurations used in this study. All model runs start at 12 UTC 27 July 2004 and the integration length is 48–54 hours. This period should cover the whole life cycle of the simulated precipitation event. In addition to operational model, a set of experimental model versions is also used (HH and NHH). The main differences to operational suites are the nonhydrostatic dynamics of NHH and partly modified physical parameterizations in both HH and NHH. The modifications in physics mainly involve changes in convection and condensation scheme (Straco, Sass, 2002) and turbulence scheme (CBR). These changes should be considered as “tuning”, which aims to make these schemes more applicable in higher resolution ($\Delta x \leq 10$ km).

Table 1: List of the conducted model runs.

Name	Δx [km]	Status	Dynamics	Physics	Boundaries
Forecasts:					
RCR	22	oper (H6.2.1)	HPE	oper	ECMWF (fc)
MBE	9	pre-oper (H6.2.1)	HPE	oper	RCR (fc)
HH	5.6	exp	HPE	mod. Straco,CBR	MBE (fc)
NHH	5.6	exp	AE-NH	mod. Straco,CBR	MBE (fc)
Simulations:					
HH	5.6	exp	HPE	mod. Straco,CBR	MBE (ana)
NHH	5.6	exp	AE-NH	mod. Straco,CBR	MBE (ana)
HH	2.8	exp	HPE	mod. Straco,CBR	MBE (ana)
NHH	2.8	exp	AE-NH	mod. Straco,CBR	MBE (ana)

oper = operational, pre-oper = pre-operational, exp = experimental,

HPE = hydrostatic primitive equations, AE-NH = anelastic non-hydrostatic, fc = forecast and ana = analyses

3 Results

3.1 Forecasts

Fig. 2 shows 12-hour precipitation amount [mm] accumulated during 36–48 hour forecast period. Both operational forecasts, panels a (RCR) and b (MBE), clearly misplace the low pressure center about 300 km to south-west from the observed location (see Fig. 1d). Consequently, the areas with heaviest predicted precipitation are also located in wrong place. RCR underestimates the maximum precipitation by about 20–25 mm, whereas MBE creates maximum rain fall more close to observed one. It should be emphasized that the comparison between model and radar retrieved precipitation is only suggestive mainly due to dissimilarity of the model and observation geometry. Naturally, both operative versions cannot predict as high amounts as observed in Vesanto (rain gauge measurement 122 mm in 24 hours \approx 61 mm in 12 hours).

Both experimental forecasts (5.6 km grid length) also misplace the low pressure center (panels 2c and 2d). This is a clear example of how the forecasts, with small integration domain, are “slaves” of their lateral boundaries. NHH produces similar precipitation distribution as MBE, whereas HH seems to overestimate the precipitation amount. The maximum precipitation amount produced by HH is clearly too strong.

Fig. 3a shows the time series of areal averaged 12-hour accumulated precipitation amount. The average is taken over the area shown in the Fig. 2c. MBE clearly produce more precipitation than RCR. On the average, HH and NHH forecasts behaves similarly than MBE. However, HH and NHH generate locally more intense precipitation rates compared to MBE, as shown in Fig. 2.

3.2 Simulations

Fig. 4 shows 12-hour precipitation amount [mm] accumulated during 36–48 hour simulation period. Now all the experiments locate the area of heaviest precipitation more or less in correct place. It is evident from the panels a (HH) and b (NHH) that maximum precipitation amounts of the simulations with 5.6 km grid length behave similarly with the forecast counterparts. HH clearly overestimates the precipitation amount, whereas NHH produces more realistic results (compared to Fig. 1d). In Figs. 4c and 4d (2.8 km grid length) the difference between hydrostatic and nonhydrostatic experiments is again distinct. However, the nonhydrostatic 2.8 km version produces less precipitation than its 5.6 km counterpart.

The time series of areal averaged 12-hour accumulated precipitation amount (Fig. 3b) show that after 24 hour integration, the simulations with 5.6 km produce more rain than the simulations with 2.8 km. This is mainly due to different size of the integration domain. Experiments with the 2.8 km grid length have to build up the precipitation within the averaging area, whereas in experiments with 5.6 km the precipitation rates are already strong. After 30 hour simulation the hydrostatic experiments start to produce more rain than nonhydrostatic ones.

Fig. 5 shows the instantaneous radar reflectivity fields from the model experiments (panels a–d) and the corresponding observations (panels e–f) valid at 12 UTC 29 July. Both hydrostatic experiments (a - 5.6 km and b - 2.8 km) create wide precipitation cells with strong reflectivity

(>40 dBZ), which are not observed. However, nonhydrostatic results are more congruent with observations.

Fig. 6 presents frequency distributions of radar reflectivity from both model experiments and observations. All the distributions are gathered during the 54 hour simulations. Nonhydrostatic experiments with 5.6 and 2.8 km grid length represent the distribution of moderate and strong reflectivities (>24 dBZ) very well, whereas hydrostatic models clearly overestimate. The overestimation by HH is much more prominent with the 2.8 km grid length. The difference between NHH experiments with different resolutions is smaller. However, it seems that the higher resolution NHH slightly underestimates the amount of strong reflectivities (>32 dBZ).

The amount of reflectivities below 24 dBZ is clearly overestimated by all experiments. This basically means that the model creates wider precipitation areas with weak intensity compared to observations. One reason to overestimation can be seen from Figs. 5d and 5f. Models cannot resolve highly scattered, smallest scale convective precipitation cells (in panel f). Instead, they produce smoother precipitation fields with weak intensity (panel d).

4 Conclusions

During 27–29 July 2004 extreme precipitation event swept over southern and central Finland creating flooding over large areas. Operational forecast of FMI starting from 12 UTC 27 July 2004 failed to produce high precipitation amounts at right locations. Therefore, several model forecasts and simulations of this event has been conducted in order to study the possible additional value of meso- γ -scale HIRLAM.

The low pressure system, which caused the precipitation event, was misplaced about 300 km by every forecast (operational and experimental). Therefore, the maximum precipitation amount was predicted in wrong place. However, the improvement of the resolution increased the predicted precipitation amounts, which is an indication that high resolution nonhydrostatic model has potential to catch up the strong precipitation rates.

The nonhydrostatic model with the 5.6 km grid length produces the best reflectivity distribution. Especially, the distribution of the strong reflectivity is impressive. However, hydrostatic experiments overestimate the amount of strong rain intensity. This overestimation is further increased when the grid length gets smaller. This is a clear example of the conditions where the hydrostatic assumption starts to lose its validity. The hydrostatic model does not have proper “breaking mechanism” for vertical mass flux (e.g. Weisman et al., 1997, Kato and Saito, 1995).

Reflectivity distributions produced by the nonhydrostatic model with 2.8 km and 5.6 km grid lengths are more or less similar. However, the interpretation of the results from the experiment with the 2.8 km grid length is complicated due to small integration domain, as explained in section 3.2. Consequently, the reflectivity distributions from the 2.8 km experiments are artificially skewed towards weak reflectivities.

At the moment, the physical parameterizations in HIRLAM are not in the level to be suitable for the 1 km scale modelling. Even if the Straco-scheme seems to be applicable with the 5.6 km grid length, generally grid scales between 4–10 km are extremely difficult for convection parameterization. Consequently, grid lengths about 1–3 km would be more preferable. Within this range it is possible to omit the deep convection parameterization. However, this imposes

more demands to other parameterizations such as prognostic hydrometeors, moist turbulence and better treatment of shallow convection among others.

Acknowledgments

We thank Carl Fortelius and Simo Järvenoja for giving valuable comments and guidance.

References

- Haase, G. and S. Crewell, 2000: Simulation of radar reflectivities using a mesoscale weather forecast model. *Water Resour. Res.*, **36**, 2221–2231.
- Haase, G. and C. Fortelius, 2001: Simulation of radar reflectivities using Hirlam forecasts. HIRLAM Tech. Rep. 51, SMHI, S-601 76 Norrköping, Sweden. Hirlam-5 Project, 22 pp.
- Kato, T. and K. Saito, 1995: Hydrostatic and non-hydrostatic simulations of moist convection: applicability of the hydrostatic approximation to a high-resolution model. *J. Meteor. Soc. Japan*, **73**, 59–77.
- Orlanski, I., 1975: A rational subdivision of scales for atmospheric processes. *Bull. Amer. Met. Soc.*, **56**, 527–530.
- Rööm, R., 2001: Nonhydrostatic adiabatic kernel for HIRLAM. Part I: Fundamentals of nonhydrostatic dynamics in pressure-related coordinates. HIRLAM Tech. Rep. 48, SMHI, S-601 76 Norrköping, Sweden. Hirlam-5 Project, 25 pp.
- Sass, B. H., 2002: A research version of the straco cloud scheme. DMI Tech. Rep. 02-10, Danish Meteorological Institute, DK-2001 Copenhagen, Denmark. 25 pp.
- Weisman, M. L., W. C. Skamarock and J. B. Klemp, 1997: The resolution dependence of explicitly modeled convective systems. *Mon. Wea. Rev.*, **125**, 527–548.

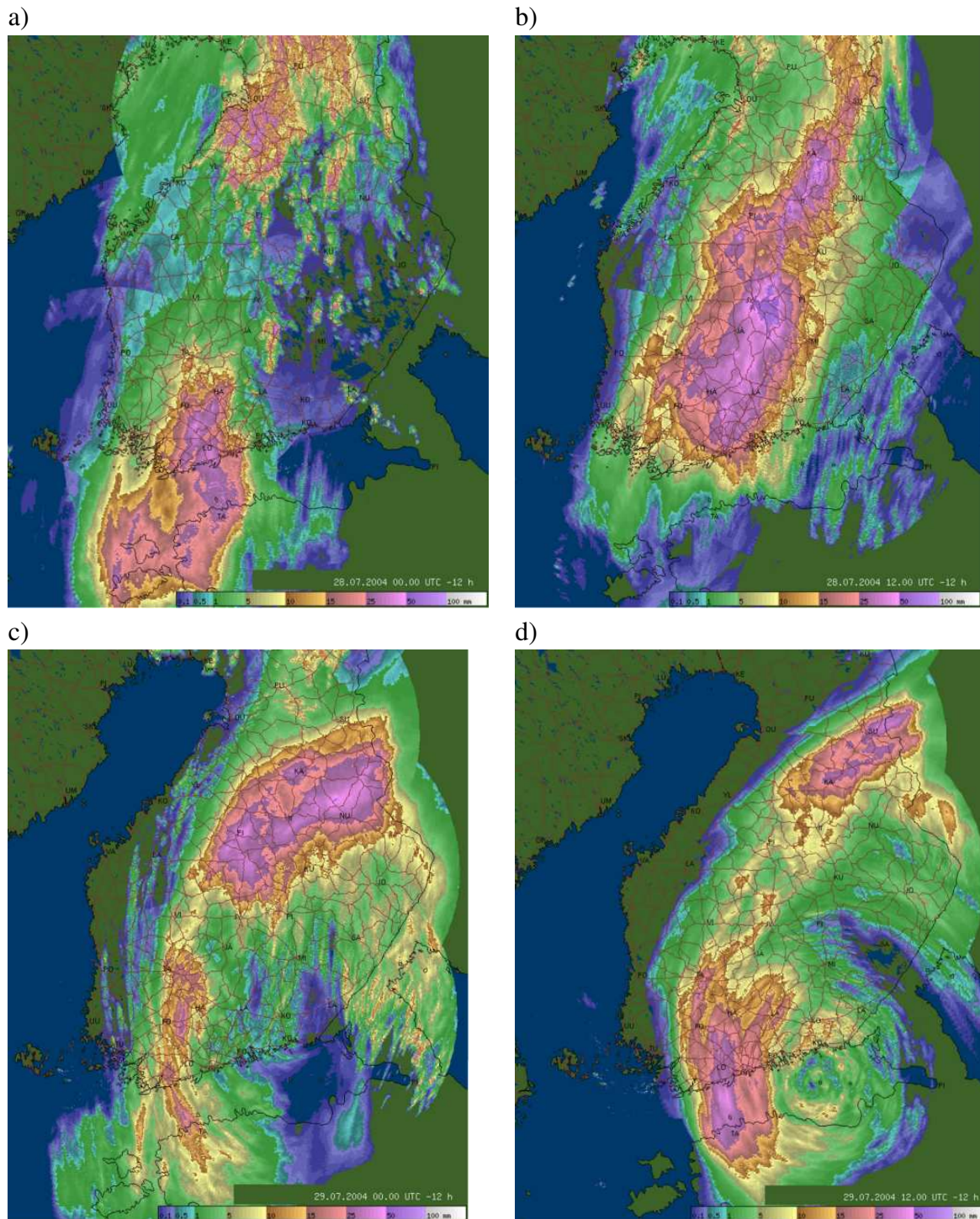
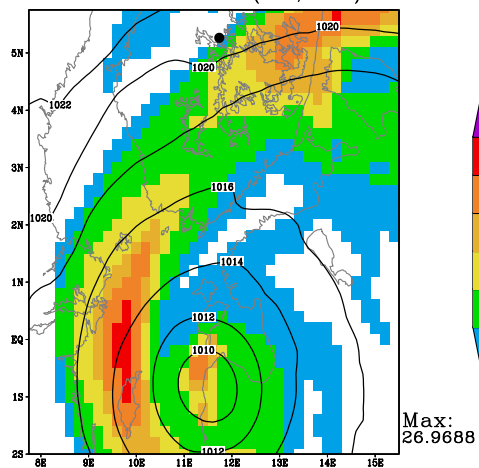


Figure 1: Accumulated 12-hour precipitation [mm] retrievals from the Finnish radar network. Valid at a) 00 UTC 28 July 2004, b) 12 UTC 28 July 2004, c) 00 UTC 29 July 2004 and d) 12 UTC 29 July 2004.

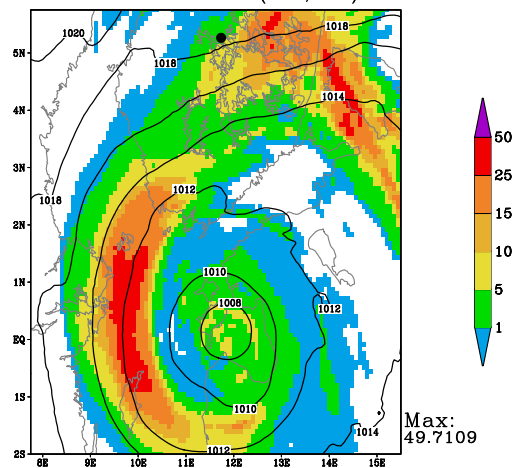
a)

HIRLAM 27JUL2004 12 UTC Forecast. Precipitation [mm/12h]
29JUL2004 12 UTC (RCR,22km)



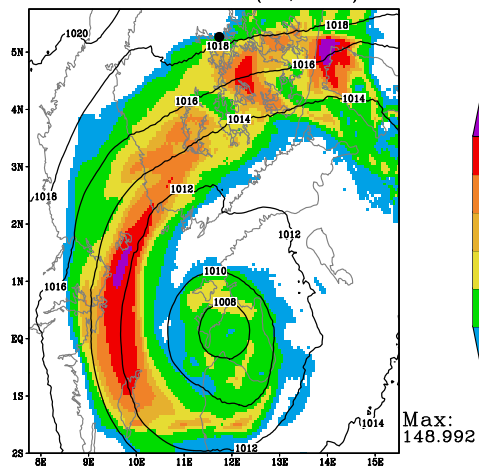
b)

HIRLAM 27JUL2004 12 UTC Forecast. Precipitation [mm/12h]
29JUL2004 12 UTC (MBE,9km)



c)

HIRLAM 27JUL2004 12 UTC Forecast. Precipitation [mm/12h]
29JUL2004 12 UTC (HH,5.6km)



d)

HIRLAM 27JUL2004 12 UTC Forecast. Precipitation [mm/12h]
29JUL2004 12 UTC (NHH,5.6km)

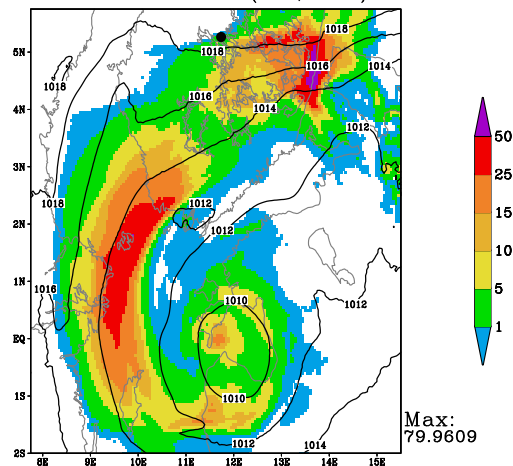
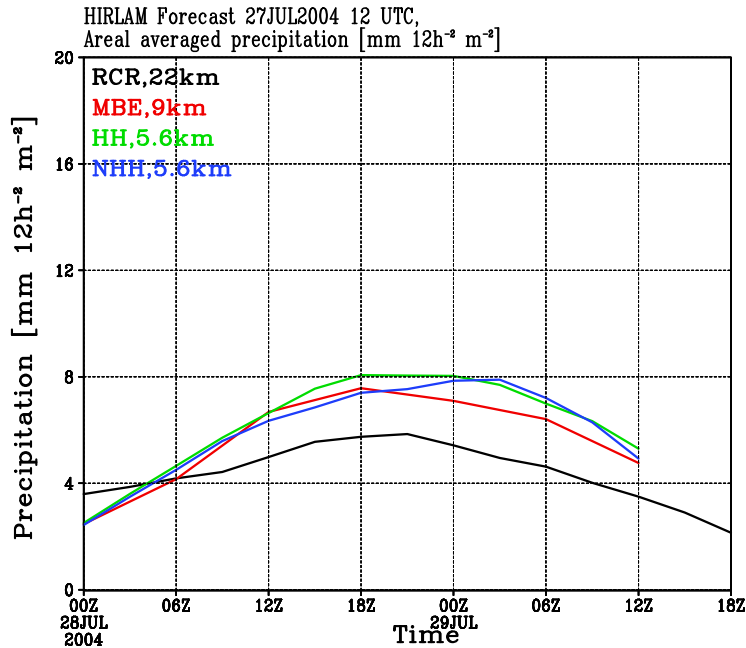


Figure 2: 48 hour forecasts (valid at 12 UTC 29 July 2004) of 12-hour accumulated precipitation [mm] and mean sea level pressure [hPa]. a) RCR, 22 km, b) MBE, 9 km, c) HH, 5.6 km and d) NHH, 5.6 km. Black dot is the location of Vesanto.

a)



b)

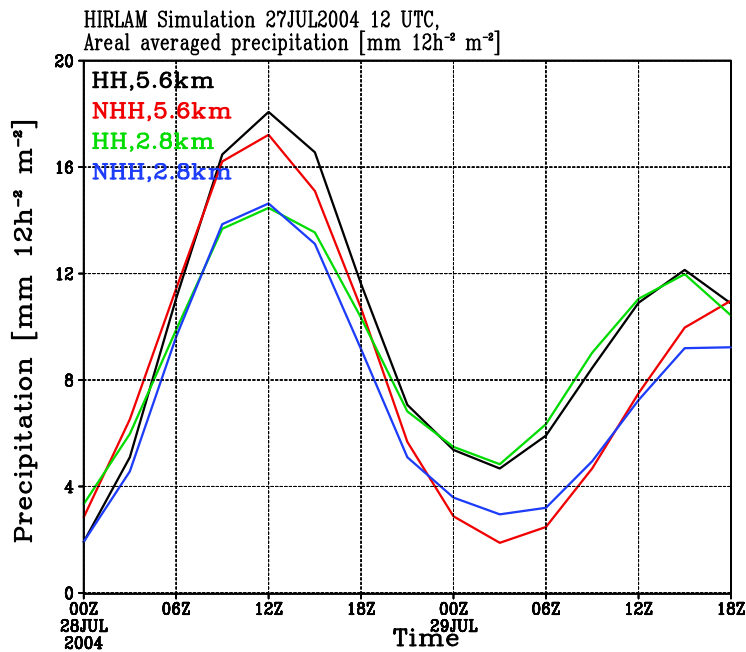
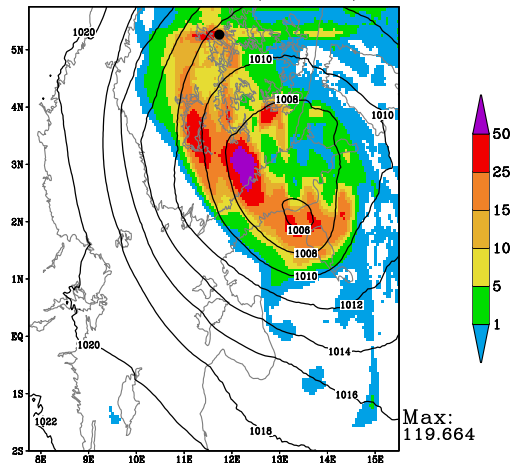


Figure 3: Time series of the areal averaged 12-hour accumulated precipitation [mm]. a) Forecasts averaged over the area seen in Fig. 2c: black = RCR, 22 km, red = MBE, 9 km, green = HH, 5.6 km and blue = NHH, 5.6 km. b) Simulations averaged over the area seen in Fig. 4c: black = HH, 5.6 km, red = NHH, 5.6 km, green = HH, 2.8 km and blue = NHH, 2.8 km.

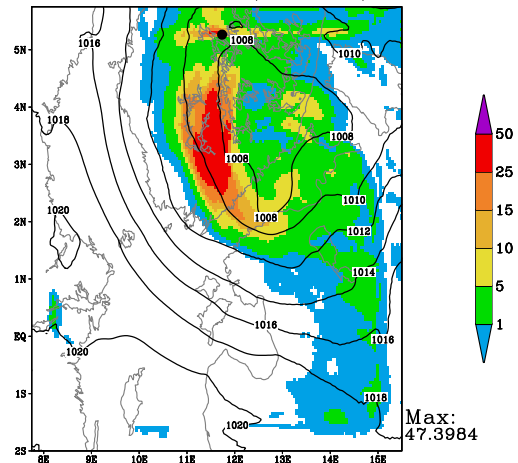
a)

HIRLAM 27JUL2004 12 UTC Simulation. Precipitation [mm/12h]
29JUL2004 12 UTC (HH,5.6km)



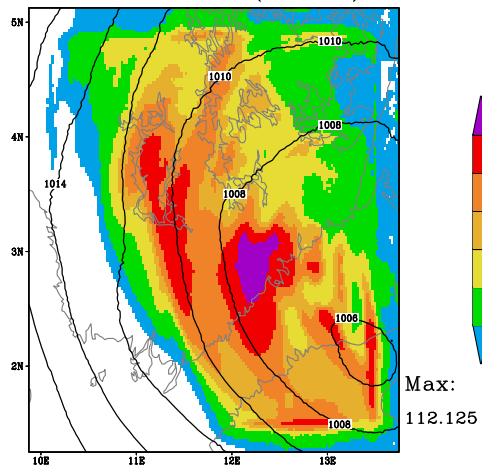
b)

HIRLAM 27JUL2004 12 UTC Simulation. Precipitation [mm/12h]
29JUL2004 12 UTC (NHH,5.6km)



c)

HIRLAM 27JUL2004 12 UTC Simulation. Precipitation [mm/12h]
29JUL2004 12 UTC (HH,2.8km)



d)

HIRLAM 27JUL2004 12 UTC Simulation. Precipitation [mm/12h]
29JUL2004 12 UTC (NHH,2.8km)

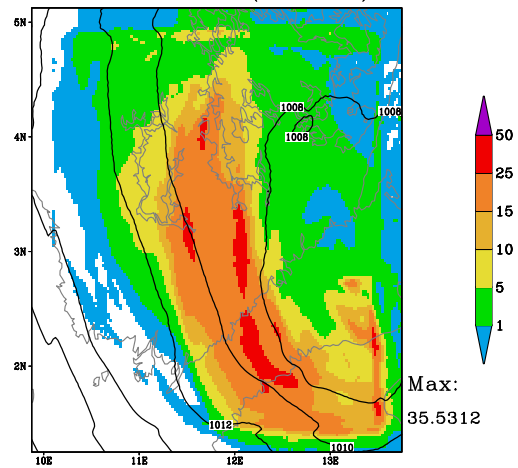


Figure 4: 48 hour simulations (valid at 12 UTC 29 July 2004) of 12-hour accumulated precipitation [mm] and mean sea level pressure [hPa]. a) HH, 5.6 km, b) NHH, 5.6 km, c) HH, 2.8 km and d) NHH, 2.8 km.

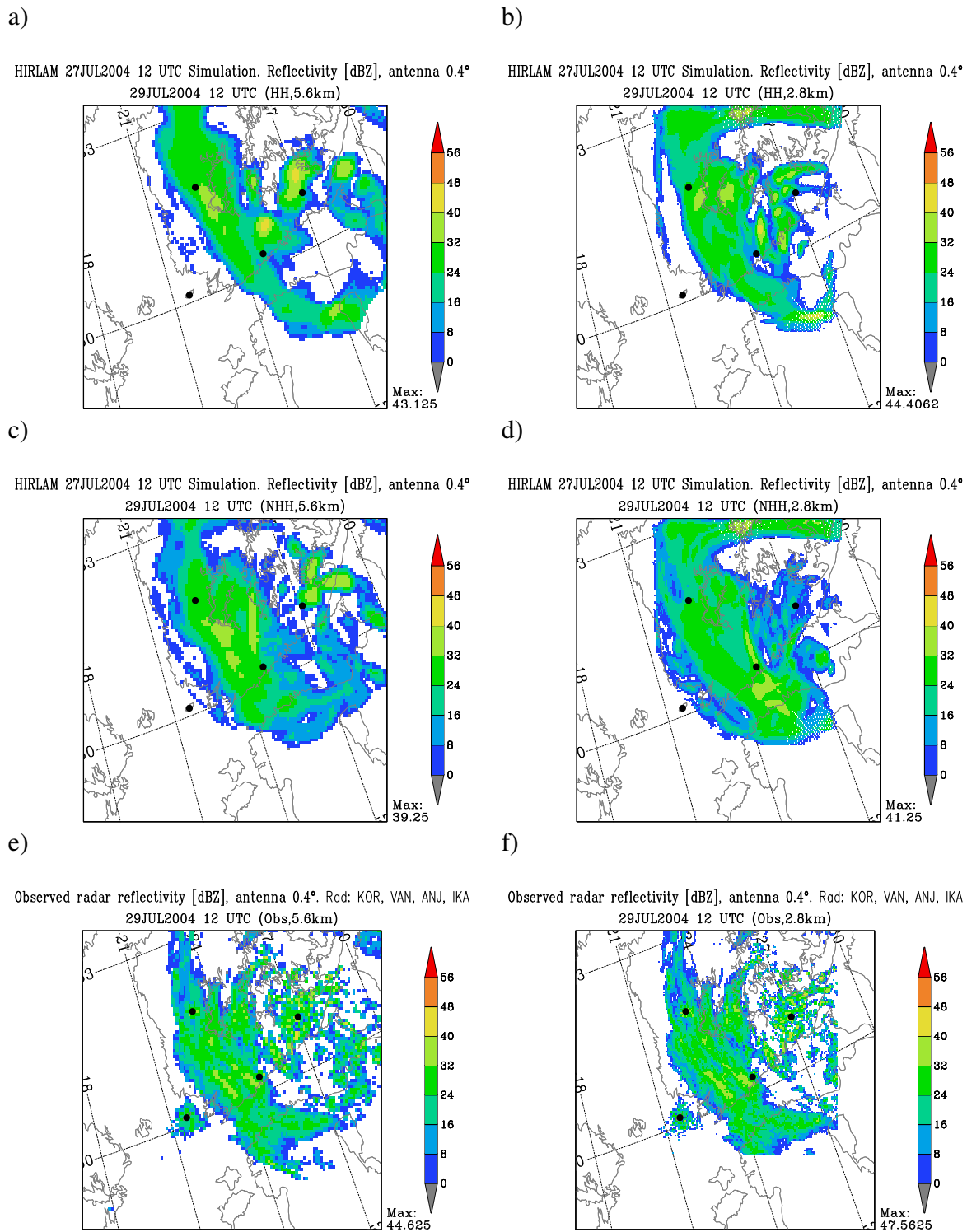
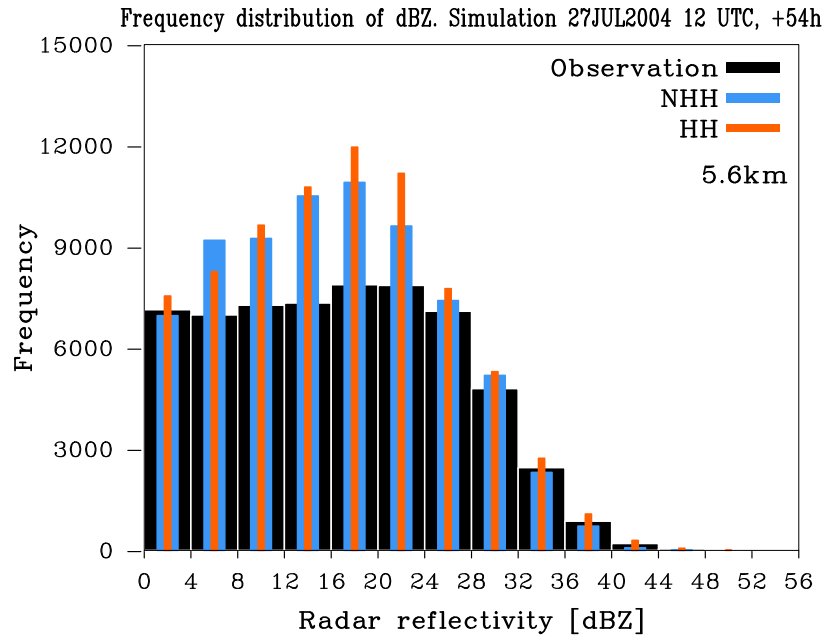


Figure 5: Composite of radar reflectivity [dBZ] fields after 48 hour simulation valid at 12 UTC 29 July 2004. a) HH, 5.6 km, b) HH, 2.8 km, c) NHH, 5.6 km, d) NHH, 2.8 km, e) radar observation, 5.6 km and f) radar observation, 2.8 km. The locations of the radars are marked with black dots.

a)



b)

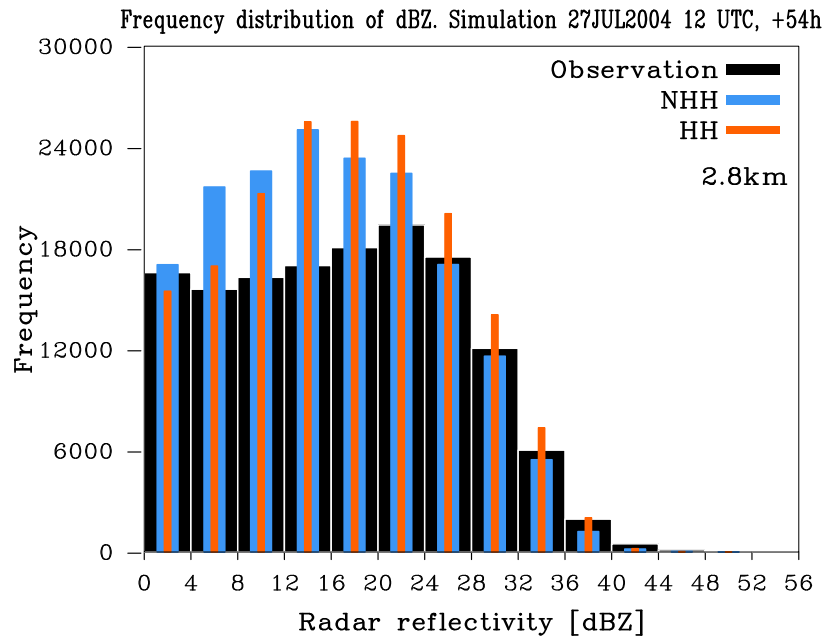


Figure 6: Frequency distributions of radar reflectivity [dBZ] produced by 54 hour simulations starting from 12 UTC 29 July 2004. Grid length is a) 5.6 km and b) 2.8 km. NHH- and HH-experiments are represented with blue and red bars, respectively. Black bars represent dBZ-observations. The elevation of radar antenna is 0.4° . In this case reflectivity values below 0 dBZ are not meteorologically important and therefore those are omitted.